ACS APPLIED MATERIALS & INTERFACES

Research Article

Cite This: ACS Appl. Mater. Interfaces 2018, 10, 17257−17268

www.acsami.org

Database for CO_2 Separation Performances of MOFs Based on Computational Materials Screening

Cigdem Altintas,[†,§] Gokay Avci,[†,§] Hilal Daglar,[†,§] Ayda Nemati Vesali Azar,[†,§] Sadiye Velioglu,[†,§] Ilknur Erucar,[‡] and Seda Keskin*[,†]

[†]Department of Chemical and Biological Engineering, Koç University, Rumelifeneri Yolu, Sariyer, 34450 Istanbul, Turkey

[‡]Department of Natural and Mathematical Sciences, Faculty of Engineering, Ozyegin University, Çekmeköy, 34794 Istanbul, Turkey

Supporting Information

ABSTRACT: Metal−organic frameworks (MOFs) are potential adsorbents for CO_2 capture. Because thousands of MOFs exist, computational studies become very useful in identifying the top performing materials for target applications in a time-effective manner. In this study, molecular simulations were performed to screen the MOF database to identify the best materials for CO_2 separation from flue gas (CO_2/N_2) and landfill gas (CO_2/CH_4) under realistic operating conditions. We validated the accuracy of our computational approach by comparing the simulation results for the CO_2 uptakes, CO_2/N_2 and CO_2/CH_4 selectivities of various types of MOFs with the available experimental data. Binary CO_2/N_2 and CO_2/CH_4 mixture adsorption data were then calculated for the entire MOF database. These data were then used to predict selectivity, working capacity, regenerability, and separation potential of MOFs. The top performing MOF adsorbents that can separate CO_2/N_2 and CO_2/CH_4 with high performance were identified. Molecular simulations for the adsorption of a ternary $CO_2/N_2/CH_4$ mixture were performed for these top materials to provide a more realistic performance assessment of MOF adsorbents. The structure−performance analysis showed that MOFs with $\Delta Q_{st}^0 > 30$ kJ/mol, 3.8 Å < pore-limiting diameter < 5 Å, 5 Å < largest cavity diameter < 7.5 Å, 0.5 < ϕ < 0.75, surface area < 1000 m^2/g, and $\rho > 1$ g/cm^3 are the best candidates for selective separation of CO_2 from flue gas and landfill gas. This information will be very useful to design novel MOFs exhibiting high CO_2 separation potentials. Finally, an online, freely accessible database https://cosmoserc.ku.edu.tr was established, for the first time in the literature, which reports all of the computed adsorbent metrics of 3816 MOFs for CO_2/N_2, CO_2/CH_4, and $CO_2/N_2/CH_4$ separations in addition to various structural properties of MOFs.

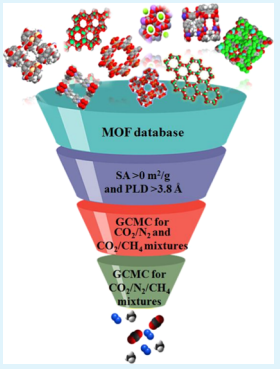

KEYWORDS: *MOF, carbon dioxide capture, flue gas separation, landfill gas separation, selectivity, molecular simulations*

1. INTRODUCTION

Metal−organic frameworks (MOFs) are crystalline nanoporous materials with various physical and chemical properties.[1] MOFs are made of metal ions connected by organic linkers to generate porous structures, and they have many interesting properties, such as ultrahigh surface areas (SAs) and very large porosities. The wide range of possibilities for the choice of metals and organic linkers has led to the development of a large number and variety of MOFs. The structural tunability of MOFs allows tailoring materials with predetermined functionalities for specific applications. MOFs have been considered to be promising for various chemical and biological applications including gas storage and separation,[2] catalysis,[3] drug storage, and delivery.[4] Among these, CO_2 separation has received significant interest because MOFs offer various pore sizes, shapes, and topologies that can be suitable for CO_2 capture.[5,6]

Development of energy-effective technologies to capture CO_2 is essential. Two separations are significant in mitigating the CO_2 emissions: (1) Flue gas separation: CO_2 capture from power plant flue gas composed mainly of N_2. (2) Landfill gas separation: CO_2 capture from natural gas composed mainly of CH_4. This purification is not only essential to increase the energy density of natural gas but also to prevent corrosion caused by the acidic CO_2 in the pipelines used to transport CH_4.[7] Activated carbons and zeolites have been tested for adsorption-based CO_2 separations. However, low selectivity and/or low regenerability of these materials caused the continuous search for new adsorbents with better performances.[8] MOFs are recently accepted as promising materials for CO_2 capture and many reviews exist on CO_2 separation using MOF adsorbents.[9−12] Several studies presented that MOFs have higher CO_2 selectivities and higher CO_2 working capacities than zeolites and carbon-based adsorbents.[13] Thousands of MOFs exist, and this large material space is an opportunity to find many appropriate MOFs that can achieve target CO_2 separations with high performance. Considering the effort, time, and resources required for the synthesis, characterization, and testing of even a single material, it is not possible to identify the best MOFs among thousands via only experimental techniques.

Received: March 21, 2018
Accepted: May 3, 2018
Published: May 3, 2018

DOI: 10.1021/acsami.8b04600
ACS Appl. Mater. Interfaces 2018, 10, 17257−17268

Molecular simulations have been shown to be useful to accurately predict the adsorption-based CO_2 separation potentials of MOFs.[14,15] We recently reviewed the large-scale simulation studies that aim to examine MOF adsorbents for CO_2 separations.[16] Watanabe and Sholl[17] performed grand canonical Monte Carlo (GCMC) simulations to calculate the adsorption isotherms of pure CO_2 and N_2 in 359 MOFs and presented ideal CO_2/N_2 selectivities at infinite dilution. Haldoupis et al.[18] studied 489 MOFs using GCMC simulations and reported ideal CO_2/N_2 selectivities at infinite dilution, which was the biggest set of estimations for adsorption-based CO_2/N_2 separation in MOFs at that time. They also examined the relations between the Henry's constants of gases and structural characteristics of MOFs. Wilmer et al.[19] calculated the adsorption of pure gases, CO_2, N_2, and CH_4, in 130 000 hypothetical MOFs using GCMC simulations. They presented the structural property−performance relations for hypothetical MOFs, which were not clearly shown for real MOFs before. Fernandez et al.[20] used machine-learning algorithms to screen the hypothetical MOFs to identify materials with enhanced CO_2 adsorption capacity. The challenge of working with hypothetical MOFs is that they may not be synthesizable in reality, and designing a synthesis procedure to make them may be very complicated. Jiang's group[21] recently used GCMC simulations to screen the CoRE MOF database (computation-ready experimental MOFs)[22] for CO_2 separation from N_2 and CH_4. They examined the quantitative relations between adsorption selectivities of MOFs and their metal types. Jimenez's group[23] recently reported a MOF database that is retained by the Cambridge Structural Database (CSD).[24] They discussed that a certain number of MOFs are missing in the CoRE MOF database and a small quantity of non-MOF materials is present. We recently screened this database using molecular simulations to recognize the best candidates for adsorption-based CH_4/H_2 separation[25] and combined GCMC simulations with molecular dynamics to identify the H_2 selective MOF membranes.[26] As far as we know, the aforementioned MOF database has not been examined for CO_2 separations.

Molecular simulations were carried out in this study to screen this most recent MOF database for identifying the most useful MOFs for CO_2 capture from flue gas and landfill gas. Adsorption data of CO_2/N_2 and CO_2/CH_4 mixtures were computed using GCMC simulations by mimicking industrial operating conditions. Binary mixture adsorption data were used to estimate well-known adsorbent selection metrics including selectivity, working capacity, adsorbent performance score (APS), sorbent selection parameter, and percent regenerability, in addition to a recently introduced metric named as the separation potential.[27] MOFs were then ranked using the combination of these metrics both for CO_2/N_2 and CO_2/CH_4 separations. Thirty top performing MOFs that can achieve CO_2 separation from these two gas mixtures with high performance were determined. GCMC simulations were then performed for these top MOFs considering ternary $CO_2/N_2/CH_4$ mixture to provide a more realistic performance assessment of MOF adsorbents. Relationships between pore size, porosity, surface area, density, lattice structure, metal type, and adsorbent selection metrics, such as selectivity and adsorbent performance score of MOFs, were investigated. These quantitative structure−performance relations are useful to make MOFs with improved CO_2/N_2 and CO_2/CH_4 separation abilities. Finally, we established an online database (https://cosmoserc.ku.edu.tr/) that reports the adsorbent selection metrics computed for every MOF for CO_2/N_2, CO_2/CH_4, and $CO_2/N_2/CH_4$ separations, in addition to CSD names and structural properties of MOFs. This database can be freely accessed and used by a large community of scientists working on MOFs for CO_2 separations. For example, experimentalists can select the MOFs by ranking the materials based on various metrics to achieve the desired CO_2 separation performances. Theoreticians can use the quantitative structure−performance information given in the database to computationally propose novel MOFs having extraordinarily good CO_2 separation capacities.

2. COMPUTATIONAL WORK

2.1. Metal−Organic Frameworks. We used the most recent MOF database integrated within the CSD.[23] This database is consisted of 54 808 non-disordered MOFs. We used a Python script from the literature[23] to clean the solvent molecules from the structures. Pore-limiting diameter (PLD), the largest cavity diameter (LCD), accessible gravimetric surface area (SA), porosity (ϕ), and density (ρ) of MOFs were computed using Zeo++ software.[28] For the pore volume and surface area calculations, a probe diameter of 0 and 3.72 Å was used, respectively. This MOF database was finally refined to eliminate MOFs having zero accessible gravimetric SAs and PLDs < 3.8 Å so that all three molecules (namely, CO_2, N_2, CH_4) can be adsorbed within the MOFs' pores. As a result, we ended up with 3816 MOFs representing extensive chemical and physical properties. Lattice and metal types of MOFs were characterized using the CSD[24] information.

2.2. Simulations Details. Grand canonical Monte Carlo (GCMC) simulations accurately compute gas uptakes in porous materials.[29] We used GCMC to calculate the adsorption data for CO_2/N_2, CO_2/CH_4, and $CO_2/N_2/CH_4$ mixtures in MOFs as implemented in the RASPA simulation code.[30] We considered CO_2/N_2: 15:85, CO_2/CH_4: 50:50, and $CO_2/N_2/CH_4$: 10:70:20 mixtures in the simulations. Compositions of the CO_2/N_2 and CO_2/CH_4 mixtures represent flue gas separation and landfill gas separation, respectively. Composition of the ternary $CO_2/N_2/CH_4$ mixture was set following the literature to represent a process for natural gas production.[31] Adsorption and desorption pressures were set as 1 and 0.1 bar, respectively, in GCMC simulations to mimic vacuum swing adsorption process.[32] The Peng−Robinson equation of state was utilized to change the pressure to the fugacity. The Lorentz−Berthelot mixing rules were used. The cutoff distance for truncation of the intermolecular interactions was set to 13 Å, and simulation cell lengths were set to at least 26 Å. Periodic boundary conditions were applied. Adsorbate−adsorbate and adsorbate−MOF interactions were defined using the Lennard-Jones (LJ) potential. In addition to LJ interactions, electrostatic interactions were considered using the Coulomb potential. To consider the electrostatic interactions between adsorbates (CO_2, N_2) having multipole moments and MOFs, partial point charges were assigned to frameworks using charge equilibration method (QEq)[33] as implemented in RASPA. The Ewald summation was implemented.[34] Ten thousand cycles were used in which the first 5000 cycles were used for initialization, and the last 5000 cycles were performed for taking ensemble averages. CO_2 molecule was modeled using a three-site rigid molecule with LJ 12−6 potential, and locations of partial point charges were set as the center of each side.[35] A three-site molecule was used for N_2, wherein two sites were

DOI: 10.1021/acsami.8b04600
ACS Appl. Mater. Interfaces 2018, 10, 17257−17268

located at the N atoms and the third site was located at the center of the mass with partial point charges.[36] Single-site spherical LJ 12−6 potential was used to model CH_4[37] molecules. Potential parameters used to describe the gas molecules can be seen in Table S1. Universal force field[38] was used for the potential parameters of MOF atoms. The good agreement between predictions of molecular simulations and experimentally reported CO_2, CH_4, and N_2 adsorptions was presented in many MOFs in our previous reports,[14,39,40] validating the accuracy of this force field. We also provided additional validations by comparing the predictions of our simulations with the experimental CO_2 uptakes and CO_2 selectivities of several MOFs, as we will discuss below. The values of isosteric heat of adsorption of gas molecules were also computed at the infinite dilution (Q_{st}^0) using the Widom particle insertion method.[29] We assumed rigid MOF structures in all of our molecular simulations to save computational time. Because the adsorbates we considered in this work are comparatively small with respect to the pore sizes of MOFs, flexibility is anticipated to have an insignificant impact on gas uptake results.[41]

2.3. Adsorbent Selection Metrics. Several different adsorbent selection metrics exist. Among these, adsorption selectivity (S), working capacity (ΔN), adsorbent performance score (APS), and percent regenerability (R%) are extensively used. These metrics were computed using the results of mixture GCMC simulations as shown in the equations given in Table 1.

Table 1. Metrics Used to Evaluate the MOF Adsorbents[a]

parameter	formula
selectivity	$S_{CO_2/i} = \frac{x_{CO_2}/x_i}{y_{CO_2}/y_i}$
working capacity	$\Delta N = N_{ads} - N_{des}$
adsorbent performance score	$APS = S_{ads,CO_2/i} \times \Delta N_{CO_2}$
percent regenerability	$R\% = \frac{\Delta N_{CO_2}}{N_{ads,CO_2}} \times 100\%$
separation potential	$\Delta Q = N_{ads,CO_2} \times \frac{y_i}{y_{CO_2}} - N_{ads,i}$

[a]i is either CH_4 or N_2 in the binary mixture. des: desorption.

The separation potential (ΔQ) was also integrated to our methodology as a new material selection criteria, which combines S and capacity in a way to demonstrate the fixed-bed adsorption process.[27] We recently showed that although selectivity has been widely used to identify the best adsorbents, MOFs with high selectivities generally have a low R%.[14] We focused on the MOFs having R% > 85% and then ranked the remaining structures based on their APSs. We focused on the top 15 MOFs having the highest APSs for CO_2/N_2 and the top 15 MOFs for CO_2/CH_4 separations. $CO_2/N_2/CH_4$ mixture simulations were only carried out for the top 30 MOFs. In this way, the best MOFs recognized in this study possess the finest combinations of S, ΔN, and R% for separation of CO_2 from both flue gas and landfill gas. This computational methodology to find the best adsorbents for binary and ternary CO_2 separation processes is shown in Figure 1. The CSD names of the MOFs together with their calculated selectivity, APS, and R% are available in our online database (https://cosmoserc.ku.edu.tr/), and users can rank the MOFs based on either of these metrics to identify the best candidates.

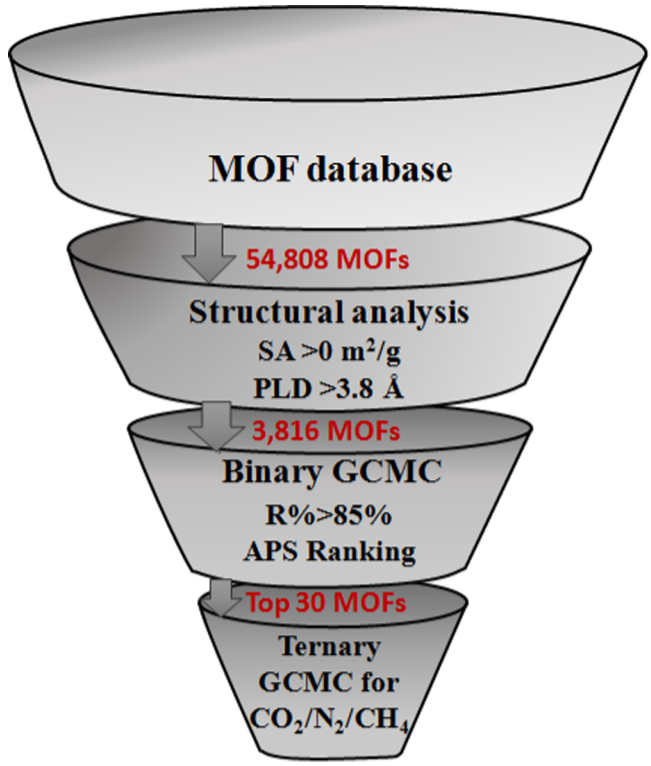

Figure 1. Computational screening methodology used in this work.

3. RESULTS AND DISCUSSION

3.1. CO_2 Separation Using MOFs. Comparison of our simulation results with the existing experiments for CO_2 uptakes, CO_2/N_2 selectivities, and CO_2/CH_4 selectivities of a large variety of MOFs including the extensively examined materials, such as IRMOF-1, CuBTC, MIL-53, MIL-100, Ni-MOF-74, UiO-66, ZIF-8, ZIF-68, and ZIF-69, is given in Figure 2. Experimental measurement conditions (pressure and temperature) for the CO_2 uptakes of MOFs, the methods used to report experimental selectivities (single-component gas/mixture/ideal adsorption theory[42]) and corresponding experimental references are given in Table S2. Figure 2 demonstrates that molecular simulations can be used to accurately define the adsorption properties of gases in various MOFs. Motivated from this, we studied the MOF database that consists of 3816 materials to examine their CO_2 separation potentials from flue gas and landfill gas mixtures. We investigated S and ΔN of MOFs for CO_2/N_2 and CO_2/CH_4 separations in Figure 3. Because CO_2 is more strongly adsorbed than CH_4 and N_2 ($CO_2 > CH_4 > N_2$), we reported selectivities and working capacities of MOFs for CO_2. CO_2 selectivities of MOFs are between 1.6−15 488 and 1.0−13 074 for CO_2/N_2 and CO_2/CH_4 mixtures, respectively. CO_2 working capacities are in the range of 0.01−4.47 and 0.02−9.57 mol/kg for CO_2/N_2 and CO_2/CH_4 mixtures, respectively. Efficient adsorbents are expected to exhibit high selectivity and high working capacity. Therefore, we used the multiplication of selectivity and working capacity as the adsorbent performance score (APS) (as described in Table 1) to describe promising MOFs.

The blue curves in Figure 3a,b represent APS = 100 and 20 for CO_2/N_2 and CO_2/CH_4 separations, respectively. Three

DOI: 10.1021/acsami.8b04600
ACS Appl. Mater. Interfaces 2018, 10, 17257−17268

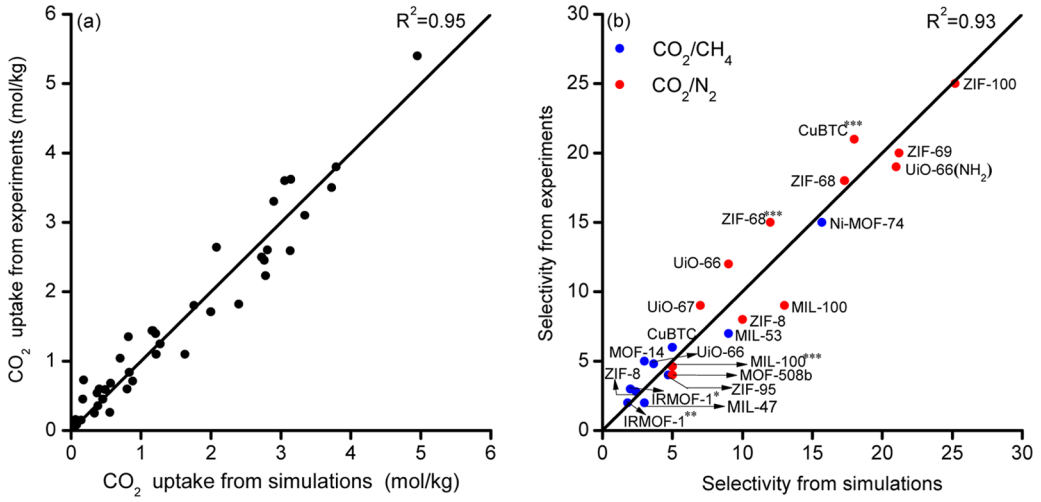

Figure 2. Comparison of our molecular simulations and experimental data for (a) CO_2 uptake (b) CO_2/CH_4 and CO_2/N_2 selectivities of MOFs. Details of the experimental data are given in Table S2a,b.

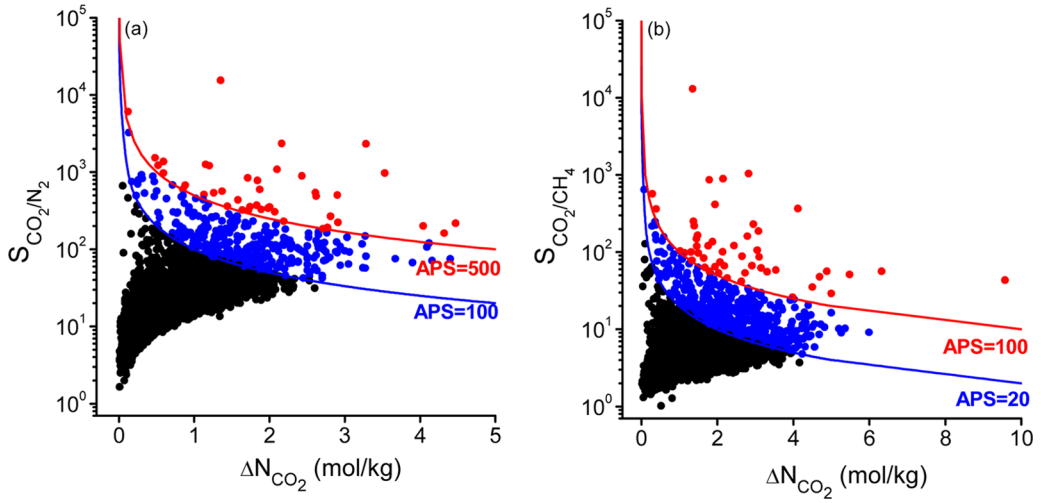

Figure 3. Selectivity (S), working capacity (ΔN), and adsorbent performance score (APS) of MOFs computed at an adsorption (desorption) pressure of 1 (0.1) bar at 298 K for (a) CO_2/N_2: 15:85 (b) CO_2/CH_4: 50:50 mixtures.

Table 2. Comparison of Zeolites and MOFs for Flue Gas and Landfill Gas Separations

material	S (CO_2/N_2)	ΔN_{CO_2} (mol/kg)	S (CO_2/CH_4)	ΔN_{CO_2} (mol/kg)	selectivity data	ref
CHA	27	3.6[a]	5.4	3.6[a]	molecular simulation: ideal selectivity, 1 bar, 300 K	52
Hβ	11.33	1.43	4.35	1.43	experiment: ideal selectivity, 1 bar, 303 K	61
ISV	6.5				molecular simulation: CO_2/N_2: 10:90, 1 bar, 308 K	52
ITE	4.8				molecular simulation: CO_2/N_2: 50:50, 1 bar, 498 K	52
MFI	20.2		2.77	0.65	molecular simulation: 50:50 for both, 1 bar, 308 K for CO_2/N_2, 303 K for CO_2/CH_4	52
MOR	35.1	0.75	10	0.8	molecular simulation: CO_2/N_2: 5:95, CO_2/CH_4: 50:50, 1 bar, 300 K	52
NaX	3000	1.2[a]	40	1.05[a]	molecular simulation: CO_2/N_2: 15:85, CO_2/CH_4: 50:50, 1 bar, 300 K	62
NaY	500	2.6[a]	30	1.7[a]	molecular simulation: CO_2/N_2: 15:85 CO_2/CH_4, 1 bar, 300 K	62
Naβ	6.34	1.15	4.12	1.15	experiment: ideal selectivity, 1 bar, 303 K	61
zeolite 13X	17.45	2.3	8.3	2.3	experiment: ideal selectivity, 1 bar, 298 K	63
zeolite 13X	14.4	1.1	6	1.3	molecular simulation: 50:50 for both, 1 bar, 298 K	64
zeolite 5A	46.5	4.18	23.5	4.18	experiment: ideal selectivity, 1 bar, 298 K	65

[a]Working capacity is calculated between 10 and 1 bar.

hundred fifty MOFs for CO_2/N_2 and 560 MOFs for CO_2/CH_4 separations exceed these curves, indicating that there are several hundreds of good adsorbent candidates. The red curves in Figure 3a,b represent APS = 500 and 100 for CO_2/N_2 and CO_2/CH_4 separations, respectively, and the MOFs that are above the red curves are the most promising materials that

DOI: 10.1021/acsami.8b04600
ACS Appl. Mater. Interfaces 2018, 10, 17257−17268

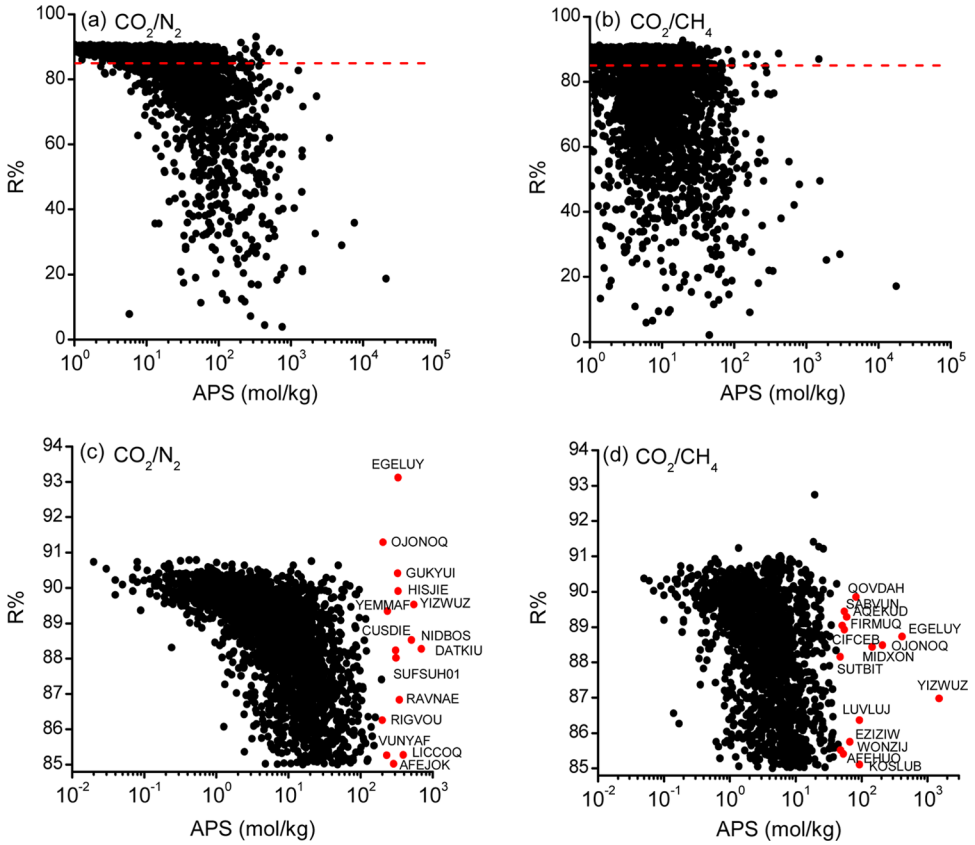

Figure 4. *R*% and APS of MOFs computed at an adsorption (desorption) pressure of 1 (0.1) bar at 298 K for (a) CO_2/N_2: 15:85 and (b) CO_2/CH_4: 50:50 mixtures. The red dotted line shows the minimum desired *R*% = 85% for (a) and (b). The red data points represent the MOFs with the highest APS and *R*% > 85 for (c) CO_2/N_2: 15:85 and (d) CO_2/CH_4: 50:50 separations.

exhibit the finest combination of selectivity and working capacity. Selectivities (working capacities) of these MOFs are between 162−15 488 (0.12−4.47 mol/kg) for CO_2/N_2 and 25−13 074 (0.29−9.57 mol/kg) for CO_2/CH_4 separations. Some of the MOFs are able to exceed the red curves due to their very high CO_2/N_2 selectivities (>1000), although they have low CO_2 working capacities (<0.6 mol/kg), as shown in Figure 3a. Similarly, several MOFs identified to be above the red curves have high CO_2/CH_4 selectivities (>300), but they have low CO_2 working capacities (<0.4 mol/kg). On the other hand, many MOFs exceed the red curves due to their moderate CO_2 selectivities (162−217 for CO_2/N_2 and 43−56 for CO_2/CH_4) and high working capacities (>4 mol/kg for CO_2/N_2 and >5 mol/kg for CO_2/CH_4). To evaluate MOFs' performance with respect to porous adsorbents, experimental and simulated gas uptakes of zeolites were found from the literature, and we reported their CO_2 selectivities and working capacities under similar operating conditions in Table 2. CO_2/N_2 selectivities of zeolites range from 3 to 3000 for CO_2/N_2 and 3 to 40 for CO_2/CH_4 separations depending on pressure, temperature, and type of measurement (single-component gas or mixture). Many MOFs outperform traditional zeolites, MFI, MOR, and zeolite 13X, in terms of CO_2/N_2 and CO_2/CH_4 selectivities. MOFs that have similar CO_2 selectivities with zeolites exhibit significantly higher working capacities, indicating that MOFs may replace zeolites in adsorption-based CO_2 separations.

We discussed that *R*% is crucial to screen MOFs in detecting the best adsorbents because many MOFs with high CO_2 selectivities have a low *R*%, which limits their practical usage in cyclic adsorption processes.[14] Therefore, we computed *R*% values for all MOFs and showed them as a function of APSs in Figure 4a,b for CO_2/N_2 and CO_2/CH_4 separations. The red dotted line in Figure 4 represents the minimum desired *R*% = 85%. Results showed that 66% of MOFs have *R*% > 85% for CO_2/N_2 separations and 45% of MOFs have *R*% > 85% for CO_2/CH_4 separations. MOFs with the highest CO_2/N_2 selectivities (>1000) suffer from low *R*% (<60%) and highly selective MOFs for CO_2/CH_4 separations (>500) have low *R*% (<40%). To efficiently identify the best adsorbents, we focused on the MOFs with *R*% > 85% and ranked them based on their APSs. Red colors represent 15 MOFs with the highest APSs and *R*% > 85% for CO_2/N_2 and CO_2/CH_4 separations in Figure 4c,d. Among these, 3 MOFs (EGELUY, OJONOQ, and YIZWUZ) are common for both gas separations. These 30 MOFs have the best combinations of selectivity, working capacity, and regenerability for efficient separation of flue gas and landfill gas.

MOFs we identified as top promising adsorbents have been already synthesized, but all of them have not been experimentally tested as adsorbents. We did a detailed literature search for the top promising materials identified in Figure 4 and found that 4 MOFs have common names together with the experimental gas adsorption data. References for experimental synthesis reports of the top materials together with the common names can be seen in Table S3. SUTBIT is known as Ni(bpb), and our simulated ideal CO_2/CH_4 selectivity of 4.82 agrees with the selectivity of ∼3 calculated from the experimental single-component adsorption isotherms of CO_2 and CH_4 in that MOF at 1 bar, 273 K.[43] SABVUN corresponds to MIL-53(Al). Our molecular simulations predicted ideal

DOI: 10.1021/acsami.8b04600
ACS Appl. Mater. Interfaces 2018, 10, 17257−17268

CO_2/N_2 selectivity of this MOF as 15.8 at 1 bar, 298 K, which agrees with the experimentally reported selectivities in the literature varying between 6 and 15 at 1 bar, 298 K.[44−47] The molecular simulations predicted CO_2 selectivity of SABVUN as 13 from an equimolar CO_2/CH_4 mixture at 5 bar, 298 K, which agrees with the experimentally reported selectivity of 7 at 5 bar, 303 K.[48] The common name of FIRMUQ is TKL-107, and our simulated CO_2/N_2 selectivity of 20 quantitatively agrees with the experimentally reported ideal selectivity of ∼11 at 1 bar, 298 K.[49] KOSLUB is known as Ni-MOF-74. Experimental CO_2/N_2 selectivity of this MOF was reported as 30 by dividing the ratio of adsorbed mass of CO_2 to N_2.[50] This corresponds to a molar selectivity of 47, which agrees well with our simulated CO_2 selectivity of 55. These comparisons showed that molecular simulations tend to slightly overestimate the experimentally reported selectivities; however, this does not alter our evaluation about CO_2 separation potential of MOFs. This comparison and the good agreement shown in Figure 2 are the direct evidences of validity of our computational screening methodology.

We also used the separation potential, ΔQ, which was recently suggested as a screening tool to choose adsorbents for multicomponent gas separations. In most of the separations analyzed by Krishna,[27] zeolite adsorbent with the highest ΔQ is not the one that has the highest selectivity. We examined the relation between ΔQ, CO_2 uptake capacity, and selectivity in Figure 5, where the size of the bubbles represents the CO_2 selectivities of MOFs. Results show that there is a correlation between these adsorbent selection metrics; ΔQ increases as the CO_2 uptake capacity of MOFs increases. Similar to zeolites, several MOFs that have very high ΔQ do not have high selectivities. For example, the MOF that offers the highest ΔQ (63 mol/L) for CO_2/N_2 separation has a high CO_2/N_2 selectivity (2321), but it is not the most selective MOF as shown in Figure 5a. The most selective MOF (HESJOE) for CO_2/N_2 separation has a lower ΔQ (40.6 mol/L) and CO_2 uptake capacity (7.17 mol/L) compared to the MOFs that have lower selectivities. Similarly, the MOF that offers the highest ΔQ (13 mol/L) and CO_2 uptake capacity (13 mol/L) for CO_2/CH_4 separation has a high selectivity (1041), but it is not the most selective MOF as presented in Figure 5b. ΔQ and CO_2 uptake capacity of zeolite NaX were reported to be the highest, 42 and 7.6 mol/L, for the separation of CO_2/N_2: 15:85 mixtures at 10 bar.[51] There are 4 MOFs that have higher ΔQ (>40 mol/L) and higher CO_2 uptake capacities (>8 mol/L) than the best-performing zeolite, indicating the potential of MOFs to replace zeolites in flue gas separations. We then examined the rankings of MOFs based on APS and ΔQ. We specifically focused on the MOFs with $R\%$ > 85% (2531 MOFs for CO_2/N_2 and 1716 MOFs for CO_2/CH_4 separations) and ranked them based on (a) APS and (b) ΔQ. To understand how well the two rankings agree with each other, the Spearman rank correlation coefficient ($-1 \leq SRCC \leq +1$) was computed. As the SRCC increases, the two rankings get closer and SRCC becomes unity when there is a perfect correlation between the two rankings. SRCC between the ranking of MOFs based on APS and the ranking based on ΔQ is 0.97 for CO_2/N_2 separation and 0.95 for CO_2/CH_4 separation, respectively. These results indicate that the two adsorbent selection metrics, APS and ΔQ, are highly correlated and can be interchangeably used to identify the best MOFs that can efficiently separate CO_2.

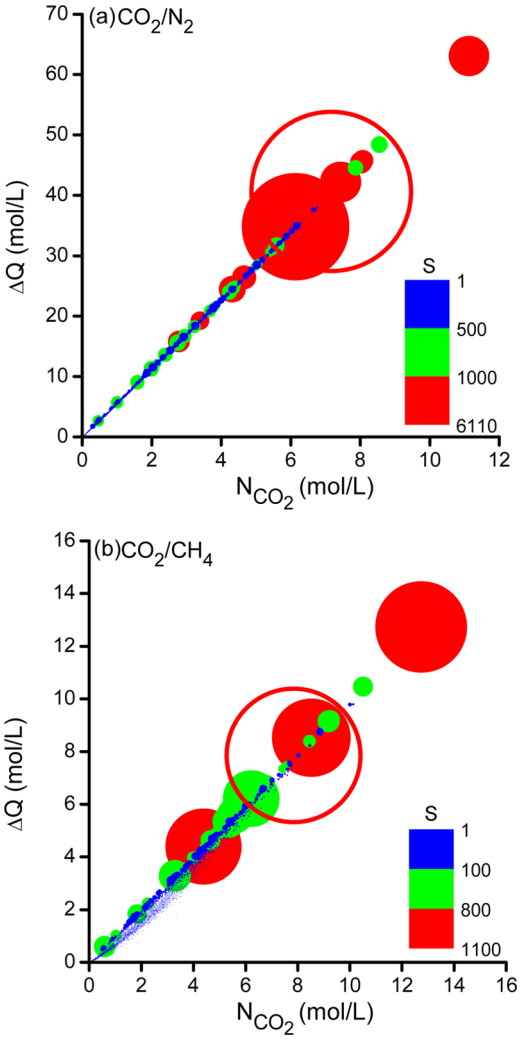

Figure 5. ΔQ, CO_2 uptake, and S of MOFs computed at an adsorption pressure of 1 bar, 298 K for (a) CO_2/N_2: 15:85 and (b) CO_2/CH_4: 50:50 separations. The size of the bubbles represents the selectivity of MOFs. The scaling factor is 0.015 in (a) and 0.075 in (b). Bubble size of the MOF with the highest selectivity was scaled with 0.009 and shown with an open circle both in (a) and (b).

Once the best MOF adsorbents were identified using the binary mixture GCMC simulations, we performed computationally demanding ternary $CO_2/N_2/CH_4$ mixture simulations for the top promising materials. Figure 6a compares the APSs of MOFs computed for two binary mixtures. APSs of MOFs computed for CO_2/N_2 mixture are generally higher than the APSs computed for CO_2/CH_4 mixture because CO_2/N_2 selectivities are generally higher than the CO_2/CH_4 selectivities. Red stars show top 12 MOFs (the ones with the highest APSs and $R\%$ > 85) for CO_2/N_2, blue stars represent the top 12 MOFs for CO_2/CH_4 separations, and 3 green stars represent the MOFs that are recognized as promising for both separations. Ternary mixture simulations were performed for these MOFs and the resulting APSs, selectivities, and working capacities were compared with those computed for binary mixtures in Figure 6b. The CO_2 working capacities predicted for ternary mixtures are lower than the ones predicted for binary mixtures, whereas CO_2 selectivities are almost the same. As a result, the APSs computed for ternary mixtures are slightly less than the ones computed for binary mixtures. The

DOI: 10.1021/acsami.8b04600
ACS Appl. Mater. Interfaces 2018, 10, 17257−17268

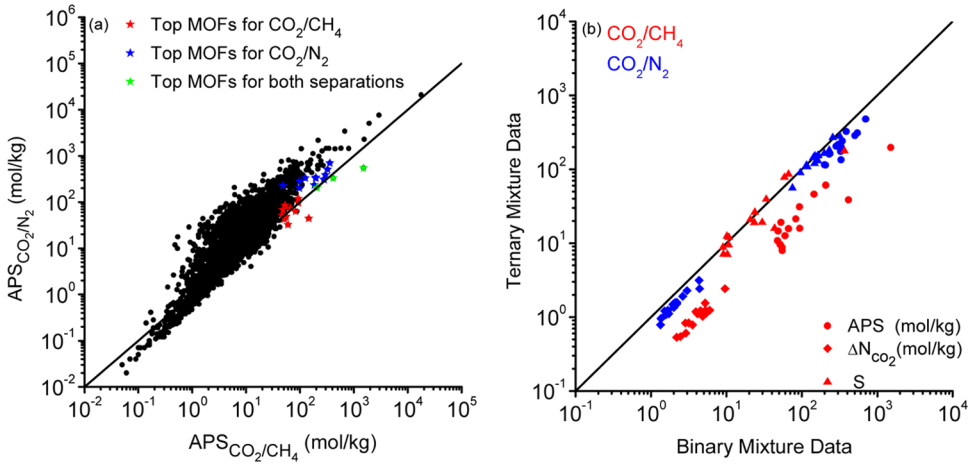

Figure 6. (a) Comparison of APSs of MOFs calculated for CO_2/N_2: 15:85 and CO_2/CH_4: 50:50 mixtures. Stars represent the top MOFs with the highest APSs. (b) Comparison of APS, ΔN, and S of MOFs calculated using binary mixture data with the ones calculated using ternary mixture data of $CO_2/N_2/CH_4$: 10:70:20.

deviations between binary and ternary APSs of MOFs are more distinct for CO_2/CH_4 due to the composition effect. Composition of CO_2 in CO_2/N_2: 15:85 mixture mimics the composition of CO_2 in ternary $CO_2/N_2/CH_4$: 10:70:20 mixture, whereas the composition of CO_2 in CO_2/CH_4: 50:50 mixture is significantly different. Ranking of the MOFs based on APSs using the binary mixture data is similar to the ranking made using the ternary mixture data. For example, the top five MOFs have the same rankings based on the binary and ternary mixture data for CO_2/N_2 mixture. For CO_2/CH_4 mixture, the first, second, third, fourth, and fifth ranked MOFs based on the binary mixture simulations rank as the first, fourth, second, third, and eight based on the ternary mixture simulations. The SRCC between APS rankings for binary mixtures and APS rankings for ternary mixtures is 0.84 for CO_2/N_2 and 0.81 for CO_2/CH_4 separations. This means molecular simulations performed for CO_2 separations from binary mixtures do a good job at estimating top MOFs for CO_2 capture from ternary mixtures. We compared the CO_2 separation performance of MOFs with zeolites for ternary mixtures. Molecular simulations reported that CO_2 uptake of zeolites MOR, CHA, and MFI are 1.5, <0.5, and <0.5 mol/kg, respectively, for a ternary $CO_2/N_2/CH_4$: 5:90:5 mixture at 300 K, 1 bar.[52] Our simulations computed CO_2 uptakes of MOFs from a $CO_2/N_2/CH_4$: 5:90:5 mixture in the range of 0.3−1.8 mol/kg at 300 K, 1 bar. Among the zeolites, CHA was reported to exhibit the highest selectivities for CO_2/N_2 (∼52) and CO_2/CH_4 (∼160) for a ternary $CO_2/N_2/CH_4$: 5:90:5 mixture at 10 bar, 300 K. To make a comparison, we performed ternary mixture GCMC simulations for the top 30 MOFs at 10 bar and calculated CO_2/N_2 selectivities of MOFs as 29.8−516.6 and CO_2/CH_4 selectivities as 8.5−339 for $CO_2/N_2/CH_4$: 5:90:5, suggesting that MOFs can beat zeolites in CO_2 separations from ternary $CO_2/N_2/CH_4$ mixtures.

3.2. Structure−Performance Relationships of MOFs.

One advantage of examining a large number of materials with varying structural and topological properties is to analyze the structure−performance relations. These relations can be helpful to lead the development of novel MOFs with better performances. In addition to easily computable structural properties, such as PLDs, LCDs, ϕ, SA, and ρ, we also analyzed the topological properties of MOFs, lattice types, and metal types because information based on these properties can be useful in directing the experimental synthesis of new MOFs. Several studies in the past focused on the relations between ΔQ_{st}^0 and MOFs' selectivities.[19,21,25,53] This property is an indicator of the interaction power between the gases and MOFs, so we included it also. We first examined the relations between ΔQ_{st}^0, PLD, LCD, ϕ, SA, ρ, and APSs of MOFs. Results did not give a clear relation, as shown in Figure S1, because APS includes both S and ΔN. MOFs with narrow pores offer a high selectivity but a low working capacity. Because APS is the multiplication of the selectivity and working capacity, MOFs with moderate APSs are either having narrow or large pores, which does not yield a clear relation between the structural properties and APS. Therefore, we aimed to define quantitative boundaries for the structural belongings of MOFs resulting in high selectivities in Figure 7. The outer circles represent all of the MOFs (3816) and the inner circles represent the top 15 most selective MOFs that offer the highest selectivity for CO_2/N_2 and CO_2/CH_4 separations at 1 bar in Figure 7a,b, respectively. Results showed that MOFs with ΔQ_{st}^0 > 30 kJ/mol, 3.8 Å < PLD < 5 Å, 5 Å < LCD < 7.5 Å, 0.5 < ϕ < 0.75, SA < 1000 m^2/g, and ρ > 1 g/cm^3 are the best adsorbents for separation of CO_2 from N_2 and CH_4. Previous work on hypothetical MOFs concluded that the most promising MOF adsorbents for CO_2/N_2 separation have 4 Å < PLDs < 8 Å and 30 kJ/mol < ΔQ_{st}^0 < 40 kJ/mol.[54] In our work, we considered real, synthesized MOFs with PLDs between 3.8 and 31 Å, and the highest selectivities for CO_2/CH_4 separation were also found to be in the same PLD (3.8 Å < PLD < 5 Å) and ΔQ_{st}^0 (30 kJ/mol < ΔQ_{st}^0 < 49 kJ/mol) region as shown in Figure 7b, indicating that there are some common structural factors between hypothetical and real MOFs. Our analysis also suggests that monoclinic MOFs are more promising. MOFs have many different metals and the most selective ones possess lanthanides and Cu for CO_2/N_2, alkali metals (Li, Na), and Cu for CO_2/CH_4 separations.

Because LCD and ϕ of MOFs seem to be more correlated with the selectivity compared to other structural properties, we examined these relations in more detail. Figure 8a represents the LCD, ϕ, and selectivity of all of the MOFs for CO_2/N_2 separations. As the porosity and LCD of MOFs decrease, selectivity represented by the bubble sizes generally increases. MOFs with selectivities >1000 are shown with open red circles and their bubble sizes are scaled with a smaller factor to have a

DOI: 10.1021/acsami.8b04600
ACS Appl. Mater. Interfaces 2018, 10, 17257−17268

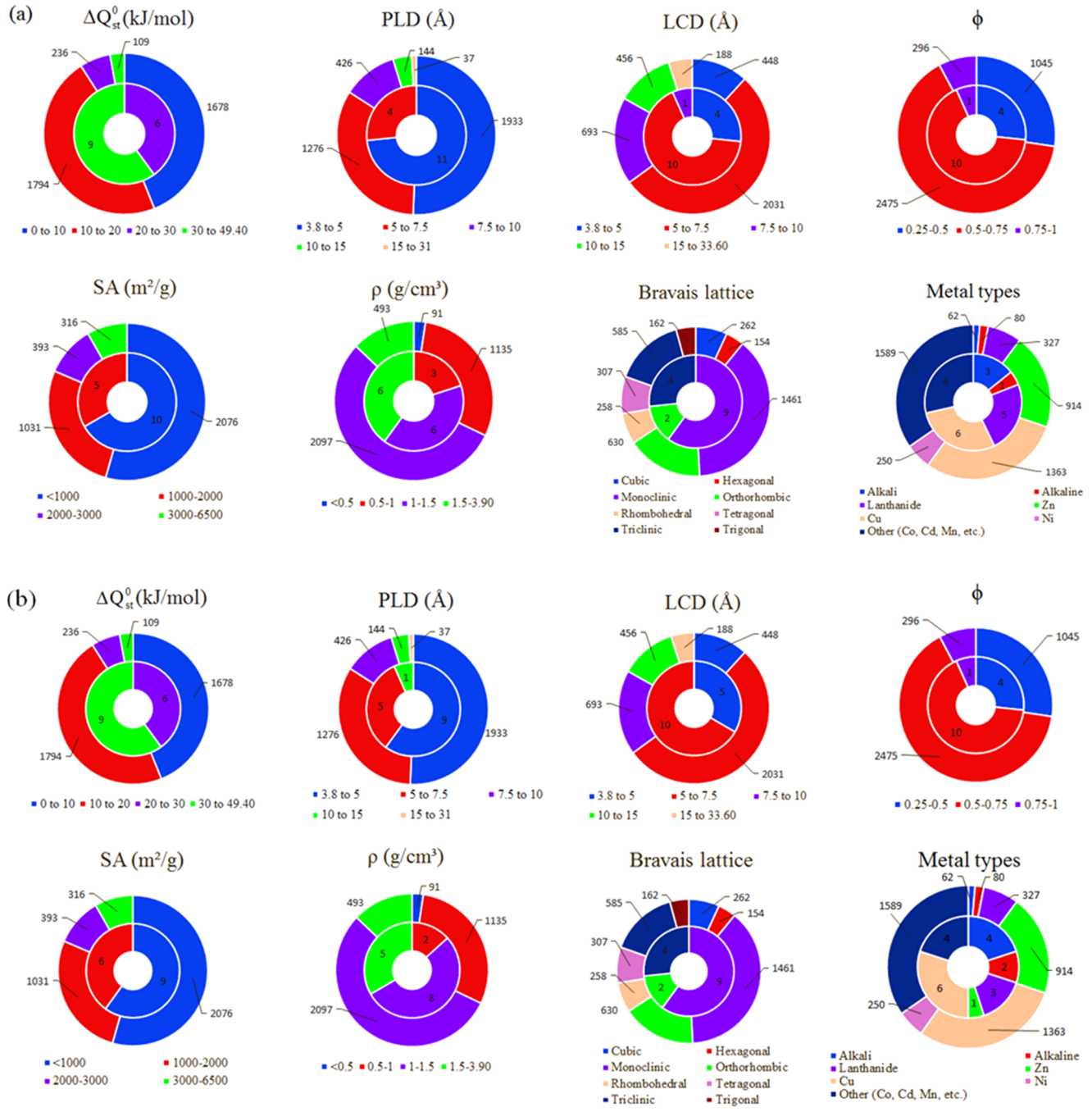

Figure 7. Effect of structural properties on the (a) CO_2/N_2 and (b) CO_2/CH_4 separation performances of MOFs. Numbers on the circles represent the number of MOFs. The outer circle represents all of the MOFs considered in this study (3816 MOFs), and the inner circle represents top 15 most promising MOFs in terms of the highest selectivities computed at 1 bar, 298 K.

clear representation in Figure 8a. The most selective MOF, HESJOE with a CO_2/N_2 selectivity of 15 488, has a low porosity (0.51) and a small LCD (4.74 Å). MOFs with selectivities >100 are shown in Figure 8b. Highly selective MOFs shown by red and green colors are generally located at the region where $\phi < 0.6$ and LCD < 6 Å. As the ϕ and LCD of MOFs decrease, the selectivities generally increase. This is due to the strong confinement of adsorbates in the narrow pores. There are a few examples that do not follow this general trend and require a more detailed analysis. For example, DOMDAL has a large LCD (18.4 Å) and a high porosity (0.79), but it exhibits a considerably high CO_2/N_2 selectivity of 543. VIHHIE, which has a relatively large LCD (6.1 Å) and a high porosity (0.77), exhibits a high CO_2/N_2 selectivity of 2321. XALROT is highly selective (1230), although it has a large LCD (7.85 Å) and a high porosity (0.65). The high selectivities of DOMDAL, VIHHIE, and XALROT can be explained by the presence of Cl^- and Br^- ions and amine groups in their structures, respectively, which increase the electrostatic interactions between the CO_2 and framework. To show this, we repeated the GCMC simulations by switching off the adsorbate−adsorbent electrostatic interactions and observed dramatic decreases in the selectivities of these MOFs. For example, the CO_2/N_2 selectivity of XALROT decreased

DOI: 10.1021/acsami.8b04600
ACS Appl. Mater. Interfaces 2018, 10, 17257−17268

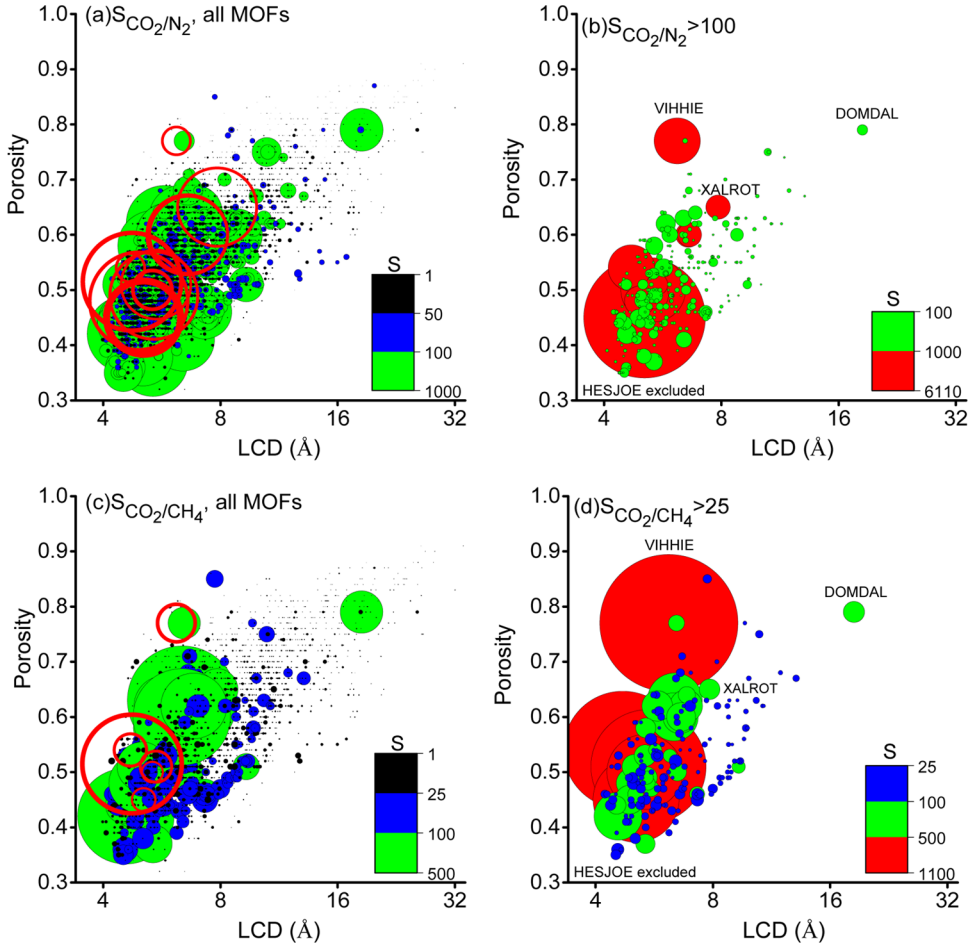

Figure 8. Relations between pore sizes, porosities, and selectivities of MOFs. The bubble size represents the selectivity of MOFs scaled with 0.06 in (a) and 0.2 in (c). Empty red circles represent the MOFs with selectivity >1000 for CO_2/N_2 in (a) and >500 for CO_2/CH_4 in (c). MOFs with CO_2/N_2 selectivities higher than 100 are shown in (b) and scaled with 0.015. MOFs with CO_2/CH_4 selectivities higher than 25 are shown in (d) and scaled with 0.1.

from 1230 to 73 and its CO_2/CH_4 selectivity decreased from 157 to 6.7. This was also supported by the decrease in ΔQ_{st}^0 values from 26 to 13 kJ/mol for CO_2/N_2 and 21 to 5 kJ/mol for CO_2/CH_4 mixture when the electrostatic interactions were neglected. Figure 8c represents all of the MOFs for CO_2/CH_4 separations and the red circles correspond to the highly selective MOFs, >500. HESJOE is the most selective MOF (13 074) due to its low LCD and porosity as discussed above. Figure 8d only shows the MOFs with CO_2/CH_4 selectivities >25 and several MOFs with selectivities >100 are generally located in the low-porosity (0.4−0.65) and narrow-LCD (4−8 Å) region, as shown with green and red colors, respectively. Similar to Figure 8b, MOFs having low porosities and narrow pores, such as HESJOE, and MOFs with specific functional groups, such as VIHHIE and DOMDAL, exhibit a high separation performance for CO_2/CH_4 separations.

Our findings indicate that it is not possible to simply correlate MOFs' CO_2 selectivities with a few structural properties. Other factors, such as the presence of specific functional groups, may also strongly affect the selectivities of MOFs. To gain more insights into the topological properties, structural similarities of the top 15 MOFs were examined by building a similarity matrix following the literature.[55,56] A similarity index was defined ($0 \leq SI \leq 1$) to provide a range of similarity measure for all of the MOFs with respect to each other. SI > 0.8 represents the most similar materials, 0.7 < SI < 0.8 shows very similar structures, 0.5 < SI < 0.7 corresponds to similar structures, 0.3 < SI < 0.5 is for the least similar structures, and 0 < SI < 0.3 shows the dissimilar MOFs. The SI analysis given in Figure S2 showed that the average SI of the top performing MOFs is 0.62 and 0.66 for flue gas and landfill gas separations, respectively, supporting the previous discussion that the top MOF adsorbents have some common structural features.

Finally, discussing the selection of charge assignment method and force fields used in our molecular simulations is important. Many different methods exist to compute the atomic charges of MOFs based on the quantum-level calculations, which are computationally demanding to perform for hundreds of MOFs. Approximate methods have been also established to assign partial charges to framework atoms, but charges from these methods are generally dissimilar.[33] It was recently shown that most of the top MOFs identified based on their CO_2/H_2O selectivities are same irrespective of the charge method.[57] We used an approximate charge calculation method (QEq) readily implemented within RASPA to screen the MOF database. The good agreement between experiments and simulations for the CO_2 uptakes and CO_2/N_2 and CO_2/CH_4 selectivities of various MOFs as we discussed above suggests that this charge assignment method accurately predicts the gas adsorption

DOI: 10.1021/acsami.8b04600
ACS Appl. Mater. Interfaces 2018, 10, 17257−17268

properties of MOFs. Highly accurate, density-derived electrostatic and chemical charge method (DDEC)[58] was used to report the partial charges of many MOFs. We repeated our GCMC simulations for the two top performing MOFs for which DDEC charges were available in the literature. Results given in Table S4 show that adsorbent selection metrics computed using QEq and DDEC are similar. For example, APS and *R*% of SABVUN were calculated as 50.14 and 90% using DDEC and 49.14 and 90.64% using QEq, respectively, for CO_2/N_2 separations. The APS and *R*% of SABVUN were calculated as 31.01 and 86.01% using DDEC and 55.08 and 89.44% using QEq for CO_2/CH_4 separations. We also performed molecular simulations using DDEC charges for additional 7 MOFs, which are not the top materials but for which DDEC charges were available in the literature. Selectivities computed with QEq and DDEC charges were found to be similar for these MOFs. It is important to note that the correlation between two charge assignment methods may change as the number of materials considered is increased. For example, Li et al.[57] observed a weak correlation (the Spearman's ranking correlation) for CO_2/N_2 selectivity between DDEC and EQEq charges. Overall, all of these results show that QEq method can be considered as an accurate and fast method for screening the MOF database to identify the promising candidates for CO_2 separations. Generic, off-the-shelf force fields may not be good in estimating CO_2 uptakes of MOFs that have open metal sites.[59,60] Specific force fields obtained from quantum chemistry calculations are needed to define the interactions between CO_2 molecules and MOFs with open metal sites. However, development of specific force fields via quantum chemistry calculations is challenging due to the computational expense and the large number of MOFs. In our work, MOFs having open metal sites may exist and may exhibit a strong CO_2 uptake, but we did not describe a specific force field for these MOFs. Throughout the article, we did not intend to discuss superiority/accuracy of the force fields, but we only aim to screen the MOF database using a generic, available force field that is valid for all varieties of MOFs to efficiently identify the best materials. Quantum chemistry calculations can be carried out for these best materials to comprehend the adsorption mechanism in detail in upcoming works. Finally, to address the effect of humidity on the CO_2 separation performances of MOFs, we also performed $CO_2/N_2/H_2O$ mixture simulations for the top 5 MOFs for flue gas separations. A comparison of CO_2/N_2 selectivities computed in the presence of humidity with the CO_2/N_2 selectivities computed for binary gas mixtures is given in Table S5. The results showed that the selectivities of MOFs computed for the ternary gas mixtures are less than those computed for binary gas mixtures, indicating that humidity decreases the CO_2/N_2 selectivities of MOFs.

4. CONCLUSIONS

In this study, the most recent and updated MOF database was screened to classify the most promising materials for flue gas and landfill gas separations. GCMC simulations were performed for CO_2/CH_4 and CO_2/N_2 mixtures, and simulation results were used to calculate important adsorbent selection metrics, such as selectivity, APS, *R*%, and ΔQ. The most promising MOFs were recognized using these metrics. Molecular simulations were then performed for these best materials to investigate the adsorption of ternary mixtures, $CO_2/N_2/CH_4$, to provide a more realistic performance assessment of MOF adsorbents. We provided the first online, freely accessible database (https://cosmoserc.ku.edu.tr/) in which the adsorbent selection metrics of MOFs for binary and ternary CO_2 separations are given. This database will be very useful to rank the MOFs based on various adsorbent selection metrics and to select the materials with desired performances. The structure−performance analysis was carried out for 3816 MOFs, and the results showed that MOFs with $\Delta Q_{st}^0 > 30$ kJ/mol, 3.8 Å < PLD < 5 Å, 5 Å < LCD < 7.5 Å, $0.5 < \phi < 0.75$, SA < 1000 m^2/g, and $\rho > 1$ g/cm^3 are the best candidates for selective separation of CO_2 from flue gas and landfill gas under vacuum swing operating conditions. This information will lead the experimental design of new MOF adsorbents to accomplish high-performance CO_2 separations.

■ ASSOCIATED CONTENT

Supporting Information

The Supporting Information is available free of charge on the ACS Publications website at DOI: 10.1021/acsami.8b04600.

Potentials used for gas molecules in molecular simulations; experimental data for CO_2 uptake and selectivity of MOFs; refcodes, common names and literature references for the top performing MOFs; comparison of gas uptakes and selectivities computed using QEq and DDEC charges; comparison of CO_2 selectivities computed for binary and ternary mixtures; effects of structural properties on the performance of MOFs with the highest APS; structural similarity indexes of the top 15 most promising MOFs (PDF)

Selectivity data of MOFs (XLSX)

■ AUTHOR INFORMATION

Corresponding Author

*E-mail: skeskin@ku.edu.tr. Phone: +90 (212) 338-1362.

ORCID

Ilknur Erucar: 0000-0002-6059-6067

Seda Keskin: 0000-0001-5968-0336

Author Contributions

[§]These authors contributed equally to this work.

Notes

The authors declare no competing financial interest.

■ ACKNOWLEDGMENTS

S.K. acknowledges ERC-2017-Starting Grant. This study has received funding from the European Research Council (ERC) under the European Union's Horizon 2020 research and innovation programme (ERC-2017-Starting Grant, grant agreement no. 756489-COSMOS).

■ REFERENCES

(1) Furukawa, H.; Cordova, K. E.; O'Keeffe, M.; Yaghi, O. M. The Chemistry and Applications of Metal-Organic Frameworks. *Science* **2013**, *341*, No. 1230444.

(2) Zornoza, B.; Tellez, C.; Coronas, J.; Gascon, J.; Kapteijn, F. Metal Organic Framework Based Mixed Matrix Membranes: An Increasingly Important Field of Research with a Large Application Potential. *Microporous Mesoporous Mater.* **2013**, *166*, 67−78.

(3) Lee, J.; Farha, O. K.; Roberts, J.; Scheidt, K. A.; Nguyen, S. T.; Hupp, J. T. Metal-Organic Framework Materials as Catalysts. *Chem. Soc. Rev.* **2009**, *38*, 1450−1459.

DOI: 10.1021/acsami.8b04600
ACS Appl. Mater. Interfaces 2018, 10, 17257−17268

(4) Erucar, I.; Keskin, S. Computational Investigation of Metal Organic Frameworks for Storage and Delivery of Anticancer Drugs. *J. Mater. Chem. B* **2017**, *5*, 7342−7351.
(5) Keskin, S.; van Heest, T. M.; Sholl, D. S. Can Metal-Organic Framework Materials Play a Useful Role in Large-Scale Carbon Dioxide Separations? *ChemSusChem* **2010**, *3*, 879−891.
(6) Li, J. R.; Ma, Y. G.; McCarthy, M. C.; Sculley, J.; Yu, J. M.; Jeong, H. K.; Balbuena, P. B.; Zhou, H. C. Carbon Dioxide Capture-Related Gas Adsorption and Separation in Metal-Organic Frameworks. *Coord. Chem. Rev.* **2011**, *255*, 1791−1823.
(7) Bae, Y.-S.; Snurr, R. Q. Development and Evaluation of Porous Materials for Carbon Dioxide Separation and Capture. *Angew. Chem., Int. Ed.* **2011**, *50*, 11586−11596.
(8) D'Alessandro, D. M.; Smit, B.; Long, J. R. Carbon Dioxide Capture: Prospects for New Materials. *Angew. Chem., Int. Ed.* **2010**, *49*, 6058−6082.
(9) Belmabkhout, Y.; Guillerm, V.; Eddaoudi, M. Low Concentration CO_2 Capture Using Physical Adsorbents: Are Metal−Organic Frameworks Becoming the New Benchmark Materials? *Chem. Eng. J.* **2016**, *296*, 386−397.
(10) Keskin, S.; van Heest, T. M.; Sholl, D. S. Can Metal-Organic Framework Materials Play a Useful Role in Large-Scale Carbon Dioxide Separations? *ChemSuschem* **2010**, *3*, 879−891.
(11) Li, J.-R.; Ma, Y.; McCarthy, M. C.; Sculley, J.; Yu, J.; Jeong, H.-K.; Balbuena, P. B.; Zhou, H.-C. Carbon Dioxide Capture-Related Gas Adsorption and Separation in Metal-Organic Frameworks. *Coord. Chem. Rev.* **2011**, *255*, 1791−1823.
(12) Lu, X.; Jin, D.; Wei, S.; Wang, Z.; An, C.; Guo, W. Strategies to Enhance CO_2 Capture and Separation Based on Engineering Absorbent Materials. *J. Mater. Chem. A* **2015**, *3*, 12118−12132.
(13) Ben-Mansour, R.; Habib, M.; Bamidele, O.; Basha, M.; Qasem, N.; Peedikakkal, A.; Laoui, T.; Ali, M. Carbon Capture by Physical Adsorption: Materials, Experimental Investigations and Numerical Modeling and Simulations−A Review. *Appl. Energy* **2016**, *161*, 225−255.
(14) Sumer, Z.; Keskin, S. Ranking of MOF Adsorbents for CO_2 Separations: A Molecular Simulation Study. *Ind. Eng. Chem. Res.* **2016**, *55*, 10404−10419.
(15) Colón, Y. J.; Snurr, R. Q. High-Throughput Computational Screening of Metal-Organic Frameworks. *Chem. Soc. Rev.* **2014**, *43*, 5735−5749.
(16) Erucar, I.; Keskin, S. High-Throughput Molecular Simulations of MOFs for CO_2 Separation: Opportunities and Challenges. *Front. Mater.* **2018**, *5*, 1−6.
(17) Watanabe, T.; Sholl, D. S. Accelerating Applications of Metal-Organic Frameworks for Gas Adsorption and Separation by Computational Screening of Materials. *Langmuir* **2012**, *28*, 14114−14128.
(18) Haldoupis, E.; Nair, S.; Sholl, D. S. Finding MOFs for Highly Selective CO_2/N_2 Adsorption Using Materials Screening Based on Efficient Assignment of Atomic Point Charges. *J. Am. Chem. Soc.* **2012**, *134*, 4313−4323.
(19) Wilmer, C. E.; Farha, O. K.; Bae, Y.-S.; Hupp, J. T.; Snurr, R. Q. Structure-Property Relationships of Porous Materials for Carbon Dioxide Separation and Capture. *Energy Environ. Sci.* **2012**, *5*, 9849−9856.
(20) Fernandez, M.; Boyd, P. G.; Daff, T. D.; Aghaji, M. Z.; Woo, T. K. Rapid and Accurate Machine Learning Recognition of High Performing Metal Organic Frameworks for CO_2 Capture. *J. Phys. Chem. Lett.* **2014**, *5*, 3056−3060.
(21) Qiao, Z.; Zhang, K.; Jiang, J. In Silico Screening of 4764 Computation-Ready, Experimental Metal−Organic Frameworks for CO_2 Separation. *J. Mater. Chem. A* **2016**, *4*, 2105−2114.
(22) Chung, Y. G.; Camp, J.; Haranczyk, M.; Sikora, B. J.; Bury, W.; Krungleviciute, V.; Yildirim, T.; Farha, O. K.; Sholl, D. S.; Snurr, R. Q. Computation-Ready, Experimental Metal-Organic Frameworks: A Tool to Enable High-Throughput Screening of Nanoporous Crystals. *Chem. Mater.* **2014**, *26*, 6185−6192.
(23) Moghadam, P. Z.; Li, A.; Wiggin, S. B.; Tao, A.; Maloney, A. G. P.; Wood, P. A.; Ward, S. C.; Fairen-Jimenez, D. Development of a Cambridge Structural Database Subset: A Collection of Metal-Organic Frameworks for Past, Present, and Future. *Chem. Mater.* **2017**, *29*, 2618−2625.
(24) Allen, F. H. The Cambridge Structural Database: A Quarter of a Million Crystal Structures and Rising. *Acta Crystallogr. B* **2002**, *58*, 380−388.
(25) Altintas, C.; Erucar, I.; Keskin, S. High-Throughput Computational Screening of the Metal Organic Framework Database for CH4/H2 Separations. *ACS Appl. Mater. Interfaces* **2018**, *10*, 3668−3679.
(26) Altintas, C.; Avci, G.; Daglar, H.; Gulcay, E.; Erucar, I.; Keskin, S. Computer Simulations of 4,240 MOF Membranes for H_2/CH_4 Separations: Insights into Structure-Performance Relations. *J. Mater. Chem. A* **2018**, 5836−5847.
(27) Krishna, R. Screening Metal-Organic Frameworks for Mixture Separations in Fixed-Bed Adsorbers Using a Combined Selectivity/Capacity Metric. *RSC Adv.* **2017**, *7*, 35724−35737.
(28) Willems, T. F.; Rycroft, C. H.; Kazi, M.; Meza, J. C.; Haranczyk, M. Algorithms and Tools for High-Throughput Geometry-Based Analysis of Crystalline Porous Materials. *Microporous Mesoporous Mater.* **2012**, *149*, 134−141.
(29) Frenkel, D.; Smit, B. *Understanding Molecular Simulation: From Algorithms to Applications*, 2nd ed.; Academic Press: San Diego, 2002.
(30) Dubbeldam, D.; Calero, S.; Ellis, D. E.; Snurr, R. Q. Raspa: Molecular Simulation Software for Adsorption and Diffusion in Flexible Nanoporous Materials. *Mol. Simul.* **2016**, *42*, 81−101.
(31) Koh, D. Y.; Ahn, Y. H.; Kang, H.; Park, S.; Lee, J. Y.; Kim, S. J.; Lee, J.; Lee, H. One-Dimensional Productivity Assessment for on-Field Methane Hydrate Production Using CO_2/N_2 Mixture Gas. *AIChE J.* **2015**, *61*, 1004−1014.
(32) Bae, Y. S.; Snurr, R. Q. Development and Evaluation of Porous Materials for Carbon Dioxide Separation and Capture. *Angew. Chem., Int. Ed.* **2011**, *50*, 11586−11596.
(33) Wilmer, C. E.; Snurr, R. Q. Towards Rapid Computational Screening of Metal-Organic Frameworks for Carbon Dioxide Capture: Calculation of Framework Charges Via Charge Equilibration. *Chem. Eng. J.* **2011**, *171*, 775−781.
(34) Ewald, P. P. Die Berechnung Optischer Und Elektrostatischer Gitterpotentiale. *Ann. Phys.* **1921**, *369*, 253−287.
(35) Potoff, J. J.; Siepmann, J. I. Vapor−Liquid Equilibria of Mixtures Containing Alkanes, Carbon Dioxide, and Nitrogen. *AIChE J.* **2001**, *47*, 1676−1682.
(36) Makrodimitris, K.; Papadopoulos, G. K.; Theodorou, D. N. Prediction of Permeation Properties of CO_2 and N_2 through Silicalite Via Molecular Simulations. *J. Phys. Chem. B* **2001**, *105*, 777−788.
(37) Martin, M. G.; Siepmann, J. I. Transferable Potentials for Phase Equilibria. 1. United-Atom Description of N-Alkanes. *J. Phys. Chem. B* **1998**, *102*, 2569−2577.
(38) Rappe, A. K.; Casewit, C. J.; Colwell, K. S.; Goddard, W. A.; Skiff, W. M. UFF, a Full Periodic Table Force Field for Molecular Mechanics and Molecular Dynamics Simulations. *J. Am. Chem. Soc.* **1992**, *114*, 10024.
(39) Sezginel, K. B.; Uzun, A.; Keskin, S. Multivariable Linear Models of Structural Parameters to Predict Methane Uptake in Metal-Organic Frameworks. *Chem. Eng. Sci.* **2015**, *124*, 125−134.
(40) Basdogan, Y.; Keskin, S. Simulation and Modelling of MOFs for Hydrogen Storage. *CrystEngComm* **2015**, *17*, 261−275.
(41) Erucar, I.; Keskin, S. Computational Assessment of MOF Membranes for CH_4/H_2 Separations. *J. Membr. Sci.* **2016**, *514*, 313−321.
(42) Myers, A. L.; Prausnitz, J. M. Thermodynamics of Mixed-Gas Adsorption. *AIChE J.* **1965**, *11*, 121−127.
(43) Galli, S.; Masciocchi, N.; Colombo, V.; Maspero, A.; Palmisano, G.; López-Garzón, F. J.; Domingo-García, M.; Fernández-Morales, I.; Barea, E.; Navarro, J. A. R. Adsorption of Harmful Organic Vapors by Flexible Hydrophobic Bis-Pyrazolate Based MOFs. *Chem. Mater.* **2010**, *22*, 1664−1672.

DOI: 10.1021/acsami.8b04600
ACS Appl. Mater. Interfaces 2018, 10, 17257−17268

(44) Camacho, B. C.; Ribeiro, R. P.; Esteves, I. A.; Mota, J. P. Adsorption Equilibrium of Carbon Dioxide and Nitrogen on the MIL-53 (Al) Metal Organic Framework. *Sep. Purif. Technol.* **2015**, *141*, 150−159.
(45) Kim, J.; Kim, W. Y.; Ahn, W.-S. Amine-Functionalized MIL-53 (Al) for CO_2/N_2 Separation: Effect of Textural Properties. *Fuel* **2012**, *102*, 574−579.
(46) Mishra, P.; Edubilli, S.; Uppara, H. P.; Mandal, B.; Gumma, S. Effect of Adsorbent History on Adsorption Characteristics of MIL-53(Al) Metal Organic Framework. *Langmuir* **2013**, *29*, 12162−12167.
(47) Pourebrahimi, S.; Kazemeini, M.; Ganji Babakhani, E.; Taheri, A. Removal of the CO_2 from Flue Gas Utilizing Hybrid Composite Adsorbent MIL-53(Al)/Gnp Metal-Organic Framework. *Microporous Mesoporous Mater.* **2015**, *218*, 144−152.
(48) Finsy, V.; Ma, L.; Alaerts, L.; De Vos, D.; Baron, G.; Denayer, J. Separation of CO_2/CH_4 Mixtures with the MIL-53 (Al) Metal−Organic Framework. *Microporous Mesoporous Mater.* **2009**, *120*, 221−227.
(49) Zhang, D.-S.; Chang, Z.; Li, Y.-F.; Jiang, Z.-Y.; Xuan, Z.-H.; Zhang, Y.-H.; Li, J.-R.; Chen, Q.; Hu, T.-L.; Bu, X.-H. Fluorous Metal-Organic Frameworks with Enhanced Stability and High H_2/CO_2 Storage Capacities. *Sci. Rep.* **2013**, *3*, No. 3312.
(50) Sumida, K.; Rogow, D. L.; Mason, J. A.; McDonald, T. M.; Bloch, E. D.; Herm, Z. R.; Bae, T.-H.; Long, J. R. Carbon Dioxide Capture in Metal−Organic Frameworks. *Chem. Rev.* **2012**, *112*, 724−781.
(51) Krishna, R. Methodologies for Screening and Selection of Crystalline Microporous Materials in Mixture Separations. *Sep. Purif. Technol.* **2018**, *194*, 281−300.
(52) García-Pérez, E.; Parra, J.; Ania, C.; Garcia-Sanchez, A.; Van Baten, J.; Krishna, R.; Dubbeldam, D.; Calero, S. A Computational Study of CO_2, N_2, and CH_4 Adsorption in Zeolites. *Adsorption* **2007**, *13*, 469−476.
(53) Wu, D.; Yang, Q. Y.; Zhong, C. L.; Liu, D. H.; Huang, H. L.; Zhang, W. J.; Maurin, G. Revealing the Structure-Property Relationships of Metal-Organic Frameworks for CO_2 Capture from Flue Gas. *Langmuir* **2012**, *28*, 12094−12099.
(54) Wilmer, C. E.; Farha, O. K.; Bae, Y. S.; Hupp, J. T.; Snurr, R. Q. Structure-Property Relationships of Porous Materials for Carbon Dioxide Separation and Capture. *Energy Environ. Sci.* **2012**, *5*, 9849−9856.
(55) Pinheiro, M.; Martin, R. L.; Rycroft, C. H.; Jones, A.; Iglesia, E.; Haranczyk, M. Characterization and Comparison of Pore Landscapes in Crystalline Porous Materials. *J. Mol. Graphics Modell.* **2013**, *44*, 208−219.
(56) Martin, R. L.; Smit, B.; Haranczyk, M. Addressing Challenges of Identifying Geometrically Diverse Sets of Crystalline Porous Materials. *J. Chem. Inf. Model.* **2012**, *52*, 308−318.
(57) Wei, L.; Zizhen, R.; Chung, Y.; Li, S. The Role of Partial Atomic Charge Assignment Methods on the Computational Screening of Metal-Organic Frameworks for CO_2 Capture under Humid Conditions. *ChemistrySelect* **2017**, *2*, 9458−9465.
(58) Manz, T. A.; Sholl, D. S. Chemically Meaningful Atomic Charges That Reproduce the Electrostatic Potential in Periodic and Nonperiodic Materials. *J. Chem. Theory Comput.* **2010**, *6*, 2455−2468.
(59) Getman, R. B.; Bae, Y. S.; Wilmer, C. E.; Snurr, R. Q. Review and Analysis of Molecular Simulations of Methane, Hydrogen, and Acetylene Storage in Metal-Organic Frameworks. *Chem. Rev.* **2012**, *112*, 703−723.
(60) Uzun, A.; Keskin, S. Site Characteristics in Metal Organic Frameworks for Gas Adsorption. *Prog. Surf. Sci.* **2014**, *89*, 56−79.
(61) Xu, X.; Zhao, X.; Sun, L.; Liu, X. Adsorption Separation of Carbon Dioxide, Methane, and Nitrogen on Hβ and Na-Exchanged B-Zeolite. *J. Nat. Gas Chem.* **2008**, *17*, 391−396.
(62) Krishna, R.; van Baten, J. M. In Silico Screening of Metal-Organic Frameworks in Separation Applications. *Phys. Chem. Chem. Phys.* **2011**, *13*, 10593−10616.
(63) Cavenati, S.; Grande, C. A.; Rodrigues, A. E. Adsorption Equilibrium of Methane, Carbon Dioxide, and Nitrogen on Zeolite 13X at High Pressures. *J. Chem. Eng. Data* **2004**, *49*, 1095−1101.
(64) Golchoobi, A.; Pahlavanzadeh, H. Extra-Framework Charge and Impurities Effect, Grand Canonical Monte Carlo and Volumetric Measurements of $CO_2/CH_4/N_2$ Uptake on Nax Molecular Sieve. *Sep. Sci. Technol.* **2017**, *52*, 2499−2512.
(65) Saha, D.; Bao, Z.; Jia, F.; Deng, S. Adsorption of CO_2, CH_4, N_2O, and N_2 on MOF-5, MOF-177, and Zeolite 5a. *Environ. Sci. Technol.* **2010**, *44*, 1820−1826.

DOI: 10.1021/acsami.8b04600
ACS Appl. Mater. Interfaces 2018, 10, 17257−17268